Solid State Science and Technology, Vol. 11, No.1 (2003) 66-72

PHOTOPYROELECTRIC MEASUREMENT OF THERMAL DIFFUSIVITY OF SOLIDS BASED ON THE THEORY OF THERMAL WAVE INTERFEROMETRY

B.Z. Azmi, H.S. Liaw, W.M.M. Yunus, M. Hashim,
M.M. Moksin, and W.M.D.W. Yusoff.
Photoacoustic Laboratory, Department of Physics, Universiti Putra Malaysia, 43400
Serdang, Selangor Darul Ehsan, Malaysia

ABSTRACT

A standard photopyroelectric configuration was used for the measurement of thermal diffusvity of solids by considering the phenomena of thermal wave interference. The thermal wave generated within the samples will be partially reflected and transmitted upon striking at the medium boundaries. The effect of infinite multiple reflection of the thermal wave within the samples was extensively discussed by Bennett and Patty in the generation of photoacoustic signal. In this work where sample surface heating was assumed and a thermally thick condition was applied, only one thermal wave reflection back into sample was considered, that is by the top pyroelectric coating, but with a series of transmitted wave into pyroelectric film from the upper and the lower pyroelectric-coating interface in the generation of photopyroelectric signal. A normalisation procedure was used to eliminate the number of unnecessary parameters needed to be known before one can determine the thermal diffusivity of the sample. With the appropriate sample-pyroelectric detector dimension, the thermal diffusivity of any solid sample is readily being determined. The method was experimentally tested for aluminum, copper, and nickel, and the values obtained were close to the literature values.

INTRODUCTION

Recently, there has been considerable interest of pyroelectric (PE) effect in polyvinylidene diflouride (PVDF) polymer since the discovery of its strong PE coefficient by Bergman et al in 1971 as cited in ref. [1]. The low cost of PVDF film, combined with good electrical properties makes the PE sensor an excellent choice in photopyroelectric (PPE) technique.

In heat transfer analysis, the procedure for measuring thermal conductivity k is difficult and time consuming. In typical experiment, a temperature gradient across the sample has to be achieved and its sides need to be insulated. Once the sample reaches a steady state, a Differential Scanning Calorimeter (DSC) is used to measure heat flux. Considerable time is required for the specimen to reach steady state if a relatively large sample is used. The other alternative is by using a relation of

$$\alpha = \frac{k}{\rho C}, \tag{1}$$

where α is known as thermal diffusivity, C is the specific heat and ρ is the density of sample. Thermal diffusivity is the ability of material to conduct thermal energy relative to its ability to store thermal energy. Hence, by determining α, C and ρ the thermal conductivity can be determined.

In this paper, a standard PPE configuration was used for the measurement of α of solids by considering the phenomena of thermal wave interference. In the generation of PPE signal, it was assumed that only surface heating and only a few of thermal wave reflections occur in sample. α of sample was obtained by fitting experimental data with theoretical equation.

THEORY

The thermal wave generated within the sample will be partially reflected and transmitted upon striking at the boundaries of two media. The effect of infinite multiple reflection of the thermal wave within the samples was extensively discussed by Bennett and Patty in the generation of photoacoustic (PA) signal [2]. In this work, a similar approach was used to obtain the complex PPE signal by adding all the transmitted terms of thermal waves that transmitted to the PE detector, instead of the transmitted terms that transmitted to the gas in PA technique. If the tested sample is highly opaque in which the optical absorption length is much smaller than sample thickness, this approach is further simplified by considering only the heat source generated on the surface of the sample. Then, the resulting thermal wave is independent of the optical properties of the sample.

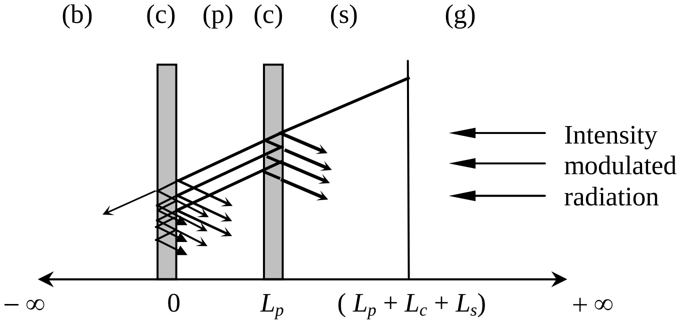

Figure 1: Thermal wave in each regions of PPE cell. The thermal waves are partially reflected and transmitted upon striking the boundaries. g, s, c, p, and b stands for gas, sample, coating, PE detector, and backing, respectively.

A one-dimensional configuration of PPE cell can be represented in Fig. 1. The thermal waves generated on surface will propagate left-wards and will be partially transmitted and reflected upon striking the interfaces of sample-coating, coating-PVDF film or shortly as coating-PE and lastly PE-coating. The reference $x = 0$ is at PE-coating interface, see Fig. 1. Generally, the thermal wave reflection coefficient R_{12} and the thermal wave transmission coefficient T_{12} at each of the interfaces are respectively given by [2,3]

$$R_{12} = \frac{1 - b_{12}}{1 + b_{12}} \quad , \qquad T_{12} = \frac{2}{1 + b_{12}}, \tag{2}$$

where b_{12} is the ratio of the thermal effusivity of the medium 2 to medium 1 for thermal wave propogate in medium 1 towards medium 2.

In thermally thick condition, consider negligible amplitude that is very small upon striking the sample-coating at second occurrence (Fig. 1). Upon striking at the first occurrence, the transmitted terms θ_s at the sample-coating interface is equal to

$$\theta_s(\omega) = \frac{Q_o}{2k_s\sigma_s} T_{sc} \exp(-\sigma_s L_s), \tag{3}$$

where Q_o is the source intensity, $\sigma_s = (1 + i)/\mu_s$, and $\mu_s = (\alpha_s/\pi f)^{1/2}$ is thermal difussion length of the sample at light modulation frequency f.

In typical PE sensor, a thin PE material is coated both sides with a very thin metallic layer acting as ohmic electrodes. Infinite multiple reflection of thermal wave is considered because of its thinness. Hence, the total transmitted terms, θ_c, at coating-PE interface is equal to

$$\theta_c(\omega) = \theta_s T_{cp} \frac{\exp(-\sigma_c L_c)}{1 - R_{cp}R_{cs} \exp(-2\sigma_c L_c)}. \tag{4}$$

The series of these transmitted thermal waves will strike the PE-coating at the bottom of PE and subsequently the series of reflected thermal waves are considered very small and died off in PE before striking the top PE-coating interface. The transmitted waves in the bottom coating will undergo infinite reflection in the coating itself and will transmit back into PE another series of transmitted wave which is the main difference from other studies [4].

The average temperature in PE, with no reflection in PE-coating interface, is given by [4]

$$\theta_p(\omega, x) = \frac{1}{L_p}\int_0^{L_p} \theta_c \exp(-\sigma_p x)\, dx. \tag{5}$$

Hence, the average temperature θ_p in the PE detector in our case where the transmitted terms from top coating and the transmitted and reflected terms from bottom coating can be written as

$$\theta_p(\omega,x) = \frac{1}{L_p}\int_0^{L_p} \theta_c \left\{ \exp(-\sigma_p x) + \exp(-2\sigma_p L_p + \sigma_p x)\left[R_{pc} + \frac{T_{pc}T_{cp}R_{cb}\exp(-2\sigma_c L_c)}{1 - R_{cp}R_{cb}\exp(-2\sigma_c L_c)} \right] \right\} \text{dx}$$

$$= \frac{\theta_c}{L_p\sigma_p}\left[1 - \exp(-\sigma_p L_p)\right]$$

$$\left\{ 1 + \left[R_{pc} + \frac{T_{pc}T_{cp}R_{cb}\exp(-2\sigma_c L_c)}{1 - R_{cp}R_{cb}\exp(-2\sigma_c L_c)} \right] \exp(-\sigma_p L_p) \right\}. \tag{6}$$

The average PE voltage is given by [5]

$$V(\omega)=\frac{pL_p\theta_p}{\varepsilon\varepsilon_o}, \tag{7}$$

where p is PE coefficient, ε is dielectric constant, and ε_o is the permittivity constant of vacuum. Thus, by using Eq. (6), the average PE voltage in our case can be written as

$$V(\omega)=\frac{Q_o p}{2\varepsilon\varepsilon_o k_s\sigma_s\sigma_p}\,\frac{T_{cp}T_{sc}\exp[-(\sigma_s L_s+\sigma_c L_c)]}{1-R_{cp}R_{cs}\exp(-2\sigma_c L_c)}\left[1-\exp(-\sigma_p L_p)\right]\times$$

$$\left\{1+\left[R_{pc}+\frac{T_{pc}T_{cp}R_{cb}\exp(-2\sigma_c L_c)}{1-R_{cp}R_{cb}\exp(-2\sigma_c L_c)}\right]\exp(-\sigma_p L_p)\right\}. \tag{8}$$

The sample α can be determined by fitting the experimental data into either the amplitude or the phase of Eq. 8. However, a number of literature values for the gas, coating, PE, and backing need to be used. A convenient way to avoid this is by normalising the signal of sample to that of reference sample. This simplify Eq. 8 to

$$\frac{V_1}{V_2}(\omega)=b_{12}\,\frac{T_{1c}}{T_{2c}}\,\frac{\exp(-\sigma_1 L_1)}{\exp(-\sigma_2 L_2)}\,\frac{1-R_{cp}R_{c2}\exp(-2\sigma_c L_c)}{1-R_{cp}R_{c1}\exp(-2\sigma_c L_c)}, \tag{9}$$

where subscript 1 and 2 represent the tested sample and reference sample, respectively.

EXPERIMENTAL PROCEDURES

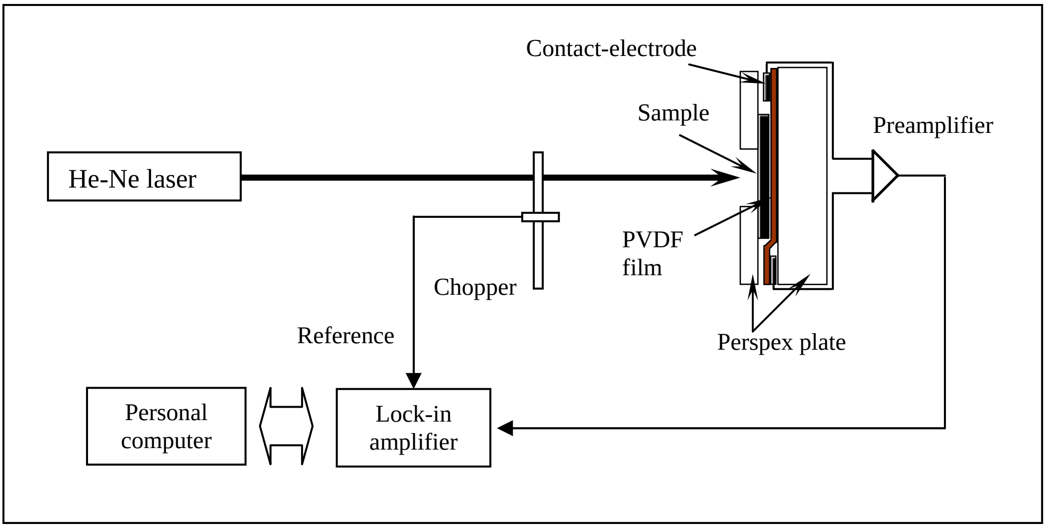

Figure 2: Schematic diagram of PPE experimental setup.

The experimental setup is shown in Figure 2. The beam from 30-mW He-Ne laser (05-LHR-991) modulated by variable frequency optical chopper (SR540) is impinged on the sample surface which in thermal contact with 36-μm-thick PVDF film supported by 1.2-cm-thick Perspex backing. A very thin layer of silver conductive grease was used as a coupling fluid to optimise the sample-detector thermal contact. The output from the PE detector was fed into a low-noise preamplifier for signal amplification and then into a lock-in amplifier (SR530) for signal analysis. A good physical contact between sample and PVDF film is achieved by pressing them in between two Perspex plates. The front plate has a circular opening to allow a direct laser beam to illuminate the sample. The measurement was carried out on aluminum, on copper, and on nickel. The measurement was recorded over a range of frequency such that the model proposed in theory section is justified.

RESULT AND DICUSSIONS

In Fig. 3, and 4, we show the unnormalised PE phase signal as a function of $f^{1/2}$ for Al (L_s = 672 μm), Cu (L_s = 944 μm), and Ni (L_s = 500 μm), where m is the slope of linearly fit line. Phase signal was chosen in present study because it does not fall off as quickly as the magnitude. The gradient caused by the infinite terms of thermal wave in the coating is in the order of 10^{-4}, which can be neglected in our following calculation of α. Thus simplify Eq. 9 to:

$$m_1 - m_2 = -\left(\frac{\pi}{\alpha_1}\right)^{1/2} L_1 + \left(\frac{\pi}{\alpha_2}\right)^{1/2} L_2 \,, \qquad (10)$$

where m_1 and m_2 are the slope of unnormalised phase signal in Fig. 3 and 4. Eq. 10 allows α of the sample to be determined directly and the calculated values of α with different material as reference sample were shown in Table 1.

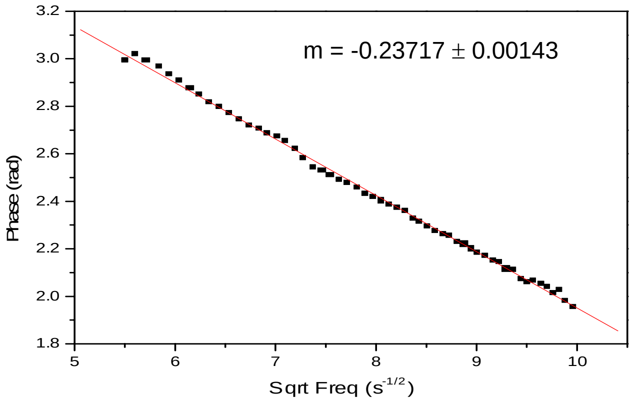

Figure 3: PPE phase signal of aluminum as a function of square root chopping frequency. The solid line represents the best-fit line with slope m.

Table 1: The obtained α values for materials used in the experiment.

Sample	Calculated α with different reference sample (cm^2s^{-1})			Literature value (cm^2s^{-1})	Reference
	Al	Cu	Ni		
Al	-	1.006	0.956	0.979, 0.933	[6,3]
Cu	1.138	-	1.117	1.163, 1.166	[6,3]
Ni	0.233	0.237	-	0.229, 0.229	[6,3]

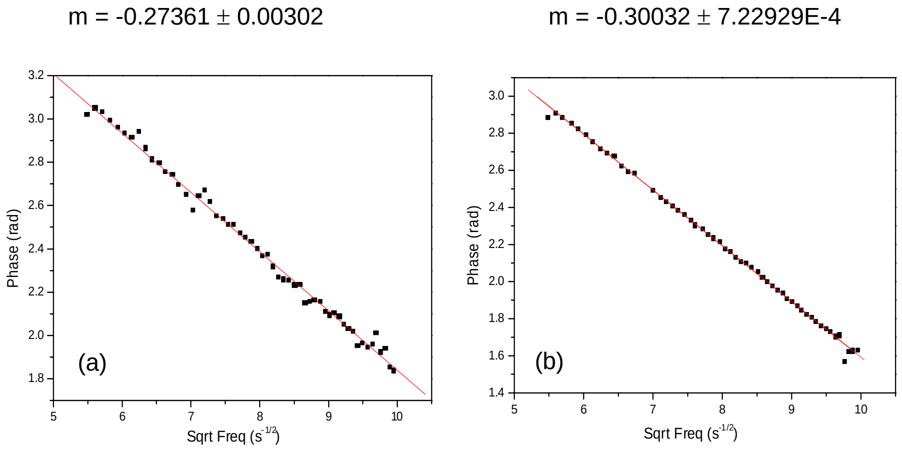

Figure 4: PPE phase signal of (a) copper and (b) nickel as a function of square root chopping frequency. The solid line represents the best-fit line with slope m.

CONCLUSION

A standard PPE configuration was used for the measurement of α of solids by considering the phenomena of single reflection of thermal wave within a sample. The thermal wave generated within the sample will be partially reflected and transmitted upon striking at the medium boundaries. An equation of complex PPE signal was derived by assuming that heating process is on the surface of the sample, single thermal wave reflection in the sample, and single reflection at the bottom coating of PE sensor. A normalisation procedure was used as a convenient way to eliminate a number of unknown parameters in other media of PPE cell. The obtained value of α for aluminum, copper, and nickel samples were close to the literature values.

ACKNOWLEDGEMENT

The authors are grateful to the Ministry of Science, Technology and the Environment of Malaysia for supporting this work under IRPA Grant No. 09-02-04-0137 and No. 02-02-04-0132-EA001.

REFERENCES

[1] Bauer, S., (1996). IEEE Transcation on Dielectrics and Electrical Insulation, **3(5)**: 647-676.
[2] Bennett, C.A. and Patty, R.R., (1982). Appl. Optics, **21**, 49-54.
[3] Almond, D.P. and Patel, P.M., (1996). Photothermal Science and Techniques, London, Chapman & Hall.
[4] Minamide, A., Shimaguchi, M., and Tokunaga, Y., (1998). Jpn. A. Appl. Phys., **37**, 3144-3147.
[5] Mandelis, A. and Zver, M. M., (1985). J Appl. Phys., **57(9)**: 4421-4430.
[6] Lide, R. D., 1997. CRC Handbook of Chemistry and Physics, 78th edition, Florida: Chemical Rubber Publishing Company.